JOURNAL OF AIRCRAFT
Vol. 36, No. 4, July–August 1999

Development of Low-Cost Differential Global Positioning System for Remotely Piloted Vehicles

Wen-Lin Guan,* Fei-Bin Hsiao,† and Ching-Shun Ho‡
National Cheng-Kung University, Tainan 701, Taiwan, Republic of China
and
Jiann-Min Huang§
Chung Shan Institute of Science and Technology, Taichung 400, Taiwan, Republic of China

The development and the application of a cost-effective differential global positioning system for remotely piloted vehicles are presented. With the aid of an aerial-photography system, i.e., digital camera and charge-coupled device camera, the low-cost global positioning system receivers (Garmin SvyII and XL-25) can perform valuable and high-accuracy positioning and navigation measurements, which are competitive with the precise (but more expensive) Ashtech Z-12 receiver. Flight-test results reveal that the low-cost payload (XL-25 system) developed can reach 10 m in spatial accuracy of the static flight trajectory and 0.17 m/s and 1 deg in accuracy for flight velocity and heading angle. The heading angle and flight-path angle can also achieve 1–3 deg rms accuracy level. Relative deviations of the rms accuracy values between XL-25 and Z-12, such as the kinematic, three-dimensional position and the flight velocity, are found to be below 2.6 m and 0.5 m/s, respectively.

Nomenclature

a	= semimajor axis of the ellipsoid
C	= speed of light
d_{ion}, d_{trop}	= ionospheric and tropospheric delay effect
$\mathrm{d}T$	= offset of the receiver clock
$\mathrm{d}t$	= offset of the satellite clock
$\mathrm{d}\rho$	= global positioning system (GPS) ephemeris error and selective availability effect error
e	= geometric flattening ratio
P	= pseudorange between the GPS satellite and the receiver
$\hat{P}_u$	= rover station's corrected pseudorange
R	= rotation parameter for coordinate transformation
S	= scale parameter for coordinate transformation
V_n, V_e, V_d	= local north, east, and down velocity of the navigation coordinate system
V_t	= navigation velocity of the flight vehicle
X, Y, Z	= world geodetic system 84 (WGS-84) coordinate system
X_m, Y_m, Z_m	= gravity center of the Taiwan datum 67 (TWD-67) coordinate system
X_u, Y_u, Z_u	= position of the GPS receiver antenna
ΔP	= GPS pseudorange correction item for differential GPS processing
ΔX, ΔY, ΔZ	= translation parameter for coordinate transformation
ε	= residual error (such as multipath effect)
ρ	= true geometric range from GPS satellite to receiver's antenna
ρ_m, ρ_P	= meridian and prime radius of curvature
ϕ, λ, h	= latitude, longitude, and altitude of the geodetic ellipsoidal coordinate system
$\dot{\phi}$, $\dot{\lambda}$	= geodetic latitude and longitude rate
Ψ, γ	= heading and flight-path angle of the flight vehicle

Subscripts

r	= GPS reference station (or base station)
u	= GPS rover station (usually the remotely piloted vehicle)

Introduction

THE Global Positioning System (GPS) has been widely used in positioning and navigation applications of flight vehicles for many years. It can continuously provide three-dimensional position, velocity, and time information under all weather conditions. However, typical horizontal and vertical positioning accuracy for a standard positioning service GPS can only reach about 100 and 150 m, respectively. The differential GPS (DGPS) was developed to improve the positioning accuracy. More precise kinematic DGPS associated with the inertial navigation system were also applied for flight navigation.[1,2] With the aid of carrier phase information in the coarse acquisition (C/A) code pseudorange data, 1-m level accuracy can be obtained. However, it is hard to solve the carrier phase observation equation for the ambiguity integer number and the cycle slip effect on the kinematic survey.[3,4]

Being lightweight and low cost, GPS is valuable for remotely piloted vehicle (RPV) autonomous flight control. Sun et al.[5] integrated GPS receivers with conventional sensors on RPVs for surveillance purposes. Sturz and Hansen[6] presented the onboard payload considerations for different RPV/unmanned air vehicle (UAV) missions. Recently, military-purpose RPVs and autonomous ground vehicles equipped with the DGPS navigation system have been widely used in many applications, such as reconnaissance, surveillance, and target acquisition.[7–9] Although the concept of using an RPV for aerial photography and remote sensing is not new, most of the aerial platforms in service are either complicated to operate or expensive because of the onboard payload equipment. For instance, the payload may include a television camera, a line scanner, an inertial measurement unit, or a data link communication module. Civilian autonomous flight-controlled RPV and GPS-based navigation system programs are also underway at some universities. The combination of DGPS and digital camera is found to perform quite well such that the onboard DGPS can provide three-dimensional position, velocity, time, and heading angle of the flight vehicle, while

Received 16 February 1998; revision received 29 March 1999; accepted for publication 29 March 1999.

*Student Ph.D. Candidate, Institute of Aeronautics and Astronautics.
†Professor, Institute of Aeronautics and Astronautics. Associate Fellow AIAA.
‡Associate Professor, Institute of Aeronautics and Astronautics.
§Associate Research Scientist, Aeronautical Research Laboratory.

Table 1 Weight, size and operation characteristics of the OS-60 RPV onboard payload

Name	Weight, kg	Dimension, cm	Characteristics	Cost, U.S.$
		Onboard system		
GPS:Survey II	0.70	15 × 10 × 5	Garmin, C/A code	1500
GPS:XL-25	0.13	8 × 5.5 × 4.5	Garmin, C/A code, L1 carrier phase	250
Air camera	0.24	11 × 6.5 × 4	SINPO-AFS10	100
CCD camera	0.31	9 × 5 × 4	SONY or Mimtron, R/S: 542 × 582 pixel	140
Digital camera	0.60	13 × 12 × 5.5	Kodak, DC-40, R/S: 760 × 506 pixel	350
Television transmiter	0.32	12.5 × 5.5 × 2	FMT-1202	500
Modem	0.40	14 × 11 × 2	TNC-220, 1200 bps	100
Battery	1.14	10 × 5 × 4 (2 sets)	5 V/12 V, 3A	25
		Ground receiving system		
GPS:Survey II	0.70		Garmin, C/A code	
Television receiver		19 × 9 × 1.5	FMR-1200	500
Television monitor				
Modem	0.40		TNC-220, 1200 bps	
Personal computer (Notebook)			Intel-486, 8 MB RAM	
Z-12	2.50	9.9 × 16 × 23	C/A, P code, L1, L2 carrier phase	3000
OS-60 RPV	4.30	1.4(l) × 2.1(w) × 0.4(h)	Futaba FP-T7UAP, OS-60 engine	750
Mission I: Svy II GPS receiver + air camera + digital DC-40 camera				1950
Mission II: XL-25 GPS receiver + DC-40 camera + CCD camera + television transmiter				1240

the digital camera or charge-coupled device (CCD) camera can be triggered synchronously with the DGPS time. Both Parkinson[4] and Montgomery[10] have successfully applied GPS technology to automatic flight control on RPV and light aviation airplanes. Not only high accuracy of 0.3 m in position and 0.1 deg in three-axis attitude angles can be obtained, but the dynamic response behaviors of the flight vehicle can be well detected. However, only a few expensive GPS receivers (usual cost around U.S.$20,000), such as Ashtech 3DF or Trimble TansVector, can provide such precise position, velocity, and attitude data.

The objective of the present study is, therefore, to develop a low-cost, easy-operating DGPS/air-photography payload system onboard an OS-60 RPV. A 10-m level dynamic accuracy is desired here. The payload includes a 35-mm camera and a digital camera (DC-40) to take the ground images, which are then integrated with the detected data of position, navigation velocity, and time from the DGPS system. During the flight tests, the RPV will carry CCD camera, radio transceiver, GPS receiver, onboard processor, and some functional supports to demonstrate the near-ground surveying and real-time position navigation. The total cost of the payload developed is well below U.S.$2000. The spatial accuracy of the present low-cost Garmin GPS receiver system is then compared with the precision Ashtech Z-12 receiver, which is of high accuracy but much more expensive in cost.

Overview of the OS-60 RPV

The OS-60 RPV is used as one of the test platforms for carrying the developed payload in the present study. The empty weight of the flight vehicle is 4.3 kg, and its wing span and body length are 1.38 and 2.1 m, respectively. The OS-60 has been flight tested to have a payload capability up to 6 kg. It is, therefore, suitable for the present study of the real-time GPS positioning and aerial CCD image transmission associated with the accessories needed in the test. For the DGPS/air-photography flight-test purpose, the equipped payload is about 4.0 kg. The major equipment loaded on the OS-60 RPV includes a GPS receiver, a set of air-photography camera and digital camera, and a radio receiver/transmitter system. Refer to Guan et al.[11] for more detailed descriptions. The onboard GPS receiver collects C/A code data to obtain navigation information and pseudorange raw data to be either recorded in the onboard memory chips or transmitted downward through a radio link for postprocessing. For the taking of ground images from the RPV, two cameras are synchronized in time with the GPS time clock, while the command of capturing the air photography is remotely controlled through the hf remotely controlled (R/C) radio link channel.

Table 1 gives the weight, size, cost, and operating characteristics of the OS-60 RPV on-board payload developed in our Remotely Piloted Vehicle and Microsatellite Research Laboratory. The DC-40 digital camera can record a total of 48 aerial images each with 756 × 504 pixels resolution. In addition, the ground control station (GCS) acts as the GPS fixed position station, RPV remote flight control, and reception of the downlink CCD image and GPS data. Figure 1 shows the block diagram of the RPV onboard payload and ground station instrumentation system.

Technique for the DGPS

Before employing the DGPS on RPV flight test, relative transformations of three reference coordinate systems are derived. They are the world geodetic system (WGS-84), the geodetic ellipsoid coordinate system (ϕ, λ, h), and a local-user coordinate system, i.e., Taiwan Datum 67 (TWD-67).

Multicoordinate Transformations

In general, most GPS use WGS-84 as a reference coordinate system. WGS-84 (X, Y, Z) is an Earth-centered, Earth-fixed (ECEF) coordinate, in which the X axis points to an associated vernal equinox, the Z axis is parallel to the Earth's rotational axis, and the Y axis is determined by the right-handed orthogonal coordinate set. The ellipsoidal coordinate (ϕ, λ, h) is a reference ellipsoid, which is approximately coincided with the mean sea level surface. The geodetic latitude angle ϕ is defined as the angle between the equatorial plane and the normal axis of the ellipsoid surface. The longitude angle λ is then the angle between the vernal equinox and the axis parallel to the equatorial plane, whereas the geodetic height h represents the reference ellipsoid. As for the TWD-67 system, its origin is located at the geological center of Taiwan (E 120°58′25.975″, N 23°58′32.34″), which is close to Wu-Zi Mountain near Pu-Li Town. In this paper, the Molodensky–Badekas (MB) model is used to implement the position transformation from WGS-84 to TWD-67 when determining the RPV flight trajectory. Relevant equations of the coordinate transformation can be written as follows:

$$\begin{bmatrix} X \\ Y \\ Z \end{bmatrix}_{\text{TWD}} = \begin{bmatrix} \Delta X \\ \Delta Y \\ \Delta Z \end{bmatrix}_{\text{MB}} + \begin{bmatrix} X_m \\ Y_m \\ Z_m \end{bmatrix} + SR \begin{bmatrix} X - X_m \\ Y - Y_m \\ Z - Z_m \end{bmatrix}_{\text{WGS-84}} \tag{1}$$

where the gravity center of the TWD-67 coordinate system is

$$\begin{bmatrix} X_m \\ Y_m \\ Z_m \end{bmatrix} = \begin{bmatrix} -03008008.169 \\ 50114376.001 \\ 2550970.447 \end{bmatrix}$$

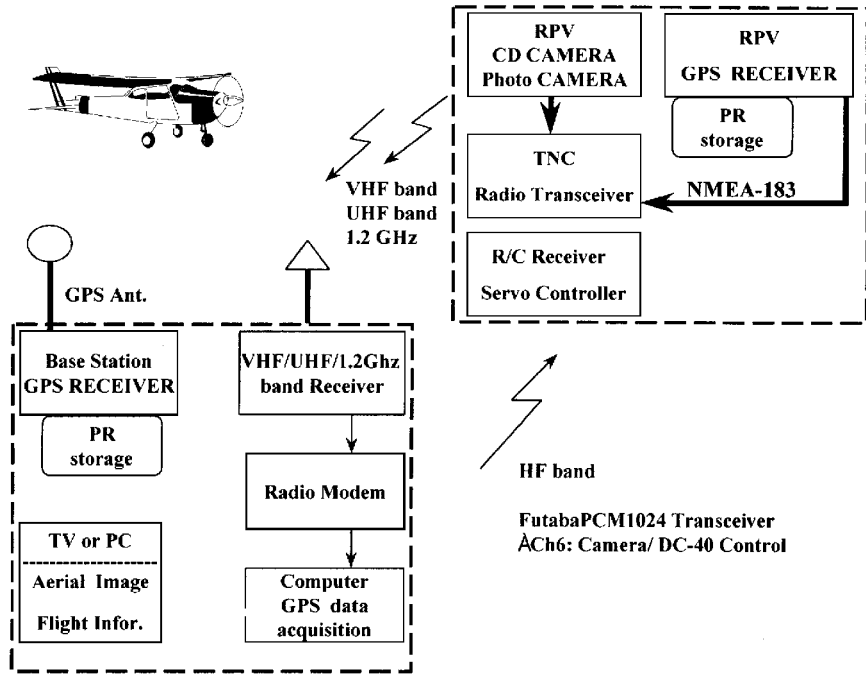

Fig. 1 Block diagram for the operation of the RPV onboard payload and GCS.

the translation parameters are

$$\begin{bmatrix} \Delta X \\ \Delta Y \\ \Delta Z \end{bmatrix} = \begin{bmatrix} 764.558 \\ 361.229 \\ 178.374 \end{bmatrix}$$

and the rotation R and scale S parameters are

$$R = \begin{bmatrix} 1 & -0.2 & 0.38 \\ 0.2 & 1 & 0.24 \\ -0.38 & -0.24 & 1 \end{bmatrix}, \qquad S = -23.29 \times 10^{-6}$$

Determination of the DGPS Position and Navigation Velocity

DGPS is a technique that can effectively improve the accuracy of GPS positioning. The base station for the DGPS is used as a reference to reduce systematic errors using the least-square scheme for detecting the flight trajectory of the flight vehicles. The errors may include satellite clock error, ionosphere and troposphere delay, receiver clock error, multipath error, etc. There are two models commonly used for GPS observation, namely, the pseudorange and the carrier phase. The pseudorange model, which is the distance between the GPS satellite and the receiver's antenna, is applied here to determine the RPV's flight trajectory and navigation velocity.

The positioning error of the flight vehicle is defined as the relative coordinate deviation between the GPS receiver onboard the vehicle (the so-called rover) and a fixed coordinate GPS receiver on the ground, i.e., the base station. Because the error sources would shift all of the time, the calculated error data from the base station should be corrected and up linked in time to the rover in the air. In mathematical modeling for such a RPV trajectory accuracy analysis, the pseudorange P can be written as

$$P = \rho + \mathrm{d}\rho + C(\mathrm{d}t - \mathrm{d}T) + d_{\mathrm{ion}} + d_{\mathrm{trop}} + \varepsilon \tag{2}$$

where ρ is the true geometry range from the GPS satellite to the receiver's antenna, i.e.,

$$\rho = \sqrt{(X_i - X_u)^2 + (Y_i - Y_u)^2 + (Z_i - Z_u)^2} \tag{3}$$

The correction term ΔP_r, obtained from the measured pseudorange, and P_r, obtained from the base station, have the relation

$$\Delta P_r = \rho_r - P_r = -[\mathrm{d}\rho_r + C(\mathrm{d}t - \mathrm{d}T_r) + d_{\mathrm{ion},r} + d_{\mathrm{trop},r} + \varepsilon_r] \tag{4}$$

The general DGPS equation for pseudorange observation is shown in Eq. (5a). Note that DGPS technique can eliminate the ephemeris errors by using a two-band GPS receiver to improve the ionospheric delay and by applying mathematical models to correct the tropospheric delay. For the case of short baseline, where the distance of the two receivers is less than about 60 km, the atmospheric delay can be neglected. Therefore, the analysis of the DGPS accuracy is only dominated by the clock deviation ΔT of the two receivers and the nondeterministic errors $\Delta\varepsilon$ (such as multipath effect, thermal noise, etc.), as shown in Eq. (5b). Hence, the corrected value of the pseudorange $\hat{P}_u$ of the rover is obtained as follows:

$$\hat{P}_u = P_u + \Delta P_r = \rho_u + (\mathrm{d}\rho_u - \mathrm{d}\rho_r) + C(\mathrm{d}T_r - \mathrm{d}T_u) + C(d_{\mathrm{ion},u} - d_{\mathrm{ion},r}) + C(d_{\mathrm{trop},u} - d_{\mathrm{trop},r}) + (\varepsilon_u - \varepsilon_r)] \tag{5a}$$

$$\hat{P}_u \approx \rho_u + C\Delta T + \Delta\varepsilon \tag{5b}$$

The equations of the flight trajectory can be further resolved by the least-square method. The subsequent data, such as the meridian radius of curvature, ρ_m; the prime radius of curvature, ρ_p; the geodetic latitude rate $\dot{\phi}$; and geodetic longitude rate $\dot{\lambda}$; can also be obtained using the following approximate formulas:

$$\rho_m = \frac{a(1-e^2)}{(1-e^2\sin^2\phi)^{1.5}} \approx a[1 + e^2(1.5\sin^2\phi - 1)] \tag{6}$$

$$\rho_p = \frac{a}{(1-e^2\sin^2\phi)^{0.5}} \approx a[1 + 0.5e^2\sin^2\phi] \tag{7}$$

where the semimajor axis of the ellipsoid (WGS-84) a is 6,378,137 m and the geometric flattening ratio $e^2 = f(2-f)$,

where $f = 1/298.2572$. The values of $\dot{\phi}$ and $\dot{\lambda}$ are directly obtained from the time difference of the GPS latitude and longitude solutions.

The determination of the navigation velocity, V_n, V_e, and V_d, is significantly affected by the noise level of the C/A code pseudorange. Although most of civilian GPS receivers can reach $3 \sim 10$ m level of position accuracy with the aid of the DGPS correction, the noise level of the pseudorangerate is still very high. This results in a poor navigation velocity error, to about 2 m/s. Therefore, it is preferable not to calculate the navigation velocity directly from the rates of latitude, longitude, and altitude data. Instead, the L1 carrier phase in association with the C/A code technique is used for the pseudorange data smoothing. The resulting accuracy is then effectively increased to the level of $10 \sim 15$ cm. The governing equations of the navigation velocity V_t and heading angle Ψ are given as follows:

$$V_t = \sqrt{V_n^2 + V_e^2 + V_d^2} \tag{8}$$

$$\Psi = \tan^{-1}(V_e/V_n) \tag{9}$$

where the relevant velocity components are

$$V_n = \dot{\phi}(\rho_m + h), \qquad V_e = \dot{\lambda}\cos\phi(\rho_p + h), \qquad V_h = -V_d = \dot{h}$$

Table 2 Comparison of the static DGPS positioning and velocity accuracy for the three receivers of Svy II, XL-25, and Z-12

	ΔE, m	ΔN, m	$\Delta\phi$, m	$\Delta\lambda$, m	ΔH, m	ΔV_n, cm/s	ΔV_e, cm/s	ΔV_h, cm/s
Static DGPS accuracy evaluation: SvyII GPS receiver								
Mean	−0.72	0.33	0.26	−0.71	−1.32	−0.01	−0.03	−0.03
Max	8.36	6.29	6.08	8.86	4.19	2.92	1.76	1.20
Min	−7.54	−5.86	−5.79	−7.88	−4.91	−1.96	−2.12	−0.90
RMS	3.50	2.18	2.12	3.67	2.52	0.76	0.75	0.35
Average PDOP = 2.7, SV = 6								
Static DGPS accuracy evaluation: XL-25 GPS receiver								
Mean	−0.06	0.08	0.07	−0.06	−0.14	−0.01	0.01	0.01
Max	5.70	8.09	7.90	6.76	7.04	0.06	0.09	0.12
Min	−7.31	−4.56	−5.22	−7.72	−11.02	−0.10	−0.09	−0.10
RMS	3.15	2.08	2.10	3.41	3.87	0.04	0.04	0.05
Average PDOP = 1.5, SV = 9								
Static DGPS accuracy evaluation: Z-12 GPS receiver								
Mean	0.00	0.00	0.00	0.00	0.00	0.00	0.03	0.01
Max	0.29	0.47	0.46	0.30	0.64	1.09	0.99	2.92
Min	−0.33	−0.37	−0.36	−0.35	−0.52	−1.21	−1.08	−4.00
RMS	0.14	0.20	0.19	0.15	0.26	0.50	0.37	1.12
Average PDOP = 2.9, SV = 7								

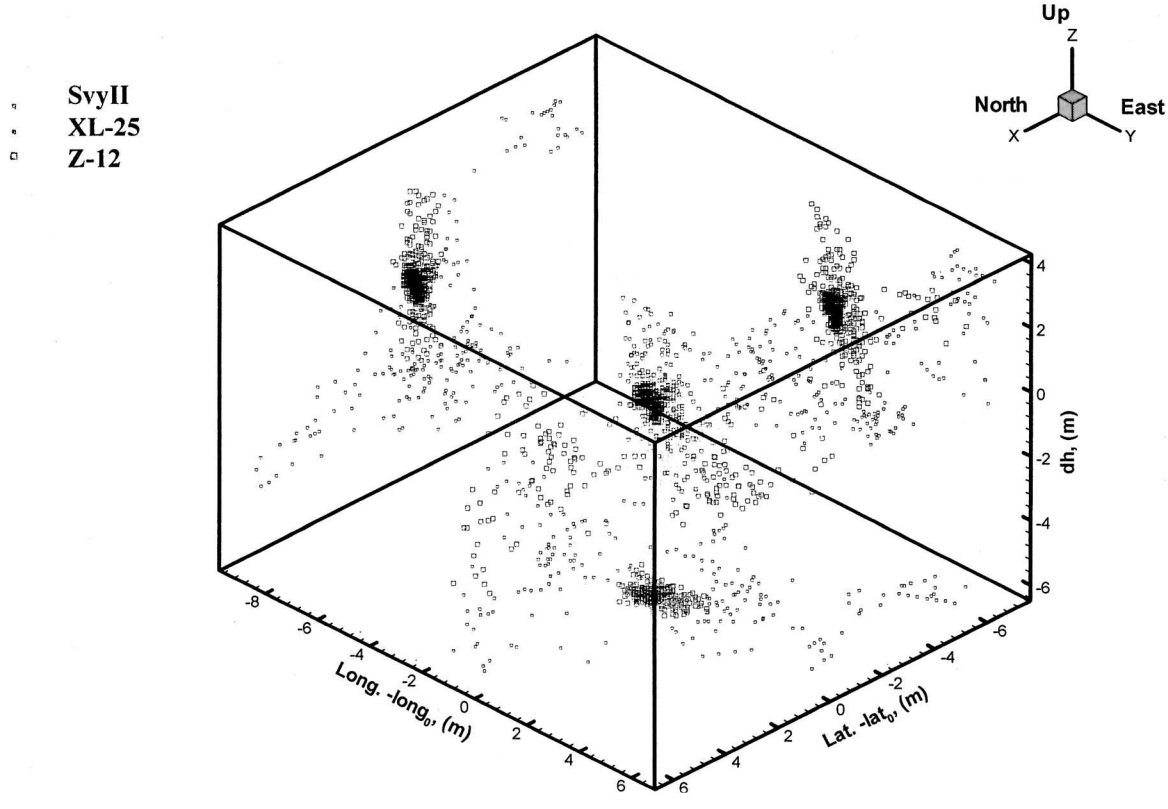

Fig. 2 Comparison of the static DGPS positioning and velocity accuracy for the three receivers of Svy II, XL-25, and Z-12.

Flight-Test Results and Discussion

Three types of GPS receivers are used, namely, Garmin Survey II (Svy II), Garmin XL-25 (XL-25), and Ashtech Z-12 (Z-12). The Svy II is a light, memory-chip-ready C/A code GPS receiver, which is applicable for real-time pseudorange data storage. The XL-25 is a card-type, easily integrated C/A code GPS receiver with L1 carrier phase tracking capability. The Z-12 with position accuracy of about 10 cm is a high-accuracy, double-band (L1 and L2) geodetic GPS receiver, which is used here mainly to provide information for ground control points corresponding to the aerial flight range. Prior to the flight test, the flight region map is established to analyze the RPV's position accuracy on the ground and to compare with the aerial image position in two- and three-dimensional coordinate systems. The AST1 GPS base station is located at $X = -2{,}962{,}826.158$, $Y = 5{,}075{,}327.313$, and $Z = 2{,}470{,}356.681$ m; $\phi = \text{N } 22^\circ 56.247954'$, $\lambda = \text{E } 120^\circ 16.507206'$, and $h = 34.91$ m. For more detailed discussion of the AST1 flight-test map and the static DGPS position analysis, refer to Guan et al.[11]

Static Accuracy Test

Static Stand-Alone GPS Accuracy Test

The standard positioning services of a stand-alone static GPS can usually provide horizontal and vertical plane accuracy to about 100 and 150 m, respectively. The single GPS position accuracy levels of Svy II, XL-25, and Z-12 are first tested on the flight vehicle and are compared to the WGS-84 ECEF and the geodetic ellipsoid coordinate systems. The results indicate that with the aid of the L1 carrier phase smoothing technique, the XL-25 can perform the pseudorange noise level to 1 m, which is lower than that of the SvyII, whose pseudorange noise level at standard C/A code is about 10–30 m. Because of the phase center shifting of the single-band patch antenna while using Svy II and XL-25, the acceleration characteristic of the flight vehicle is also observed to be difficult to measure, as compared with the double-band geodetic antenna of Z-12. In summary, the mean velocity errors of Svy II, XL-25, and Z-12 are 8.77, 1.18, and 0.37 m/s, respectively.

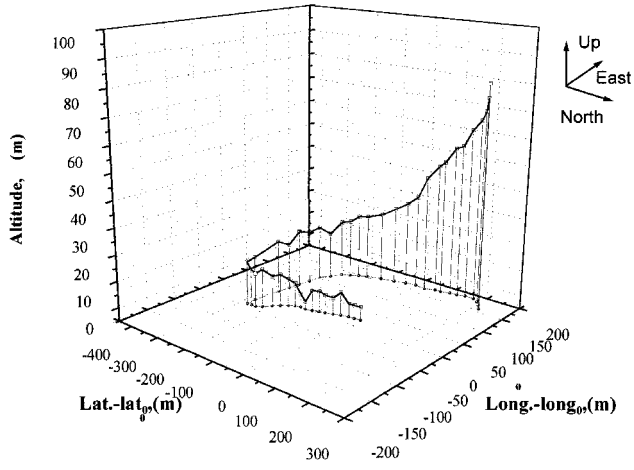

Fig. 3 Three-dimensional flight trajectory detected by Svy II DGPS for the OS-60 RPV at takeoff condition.

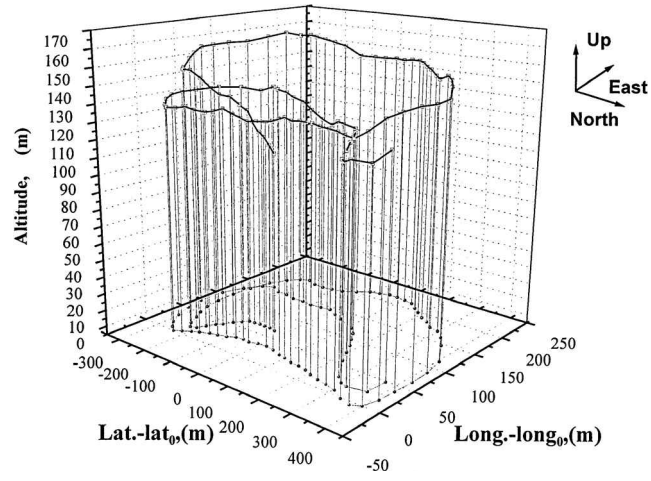

Fig. 5 Three-dimensional flight trajectory detected by Svy II DGPS for the OS-60 RPV at cruise condition.

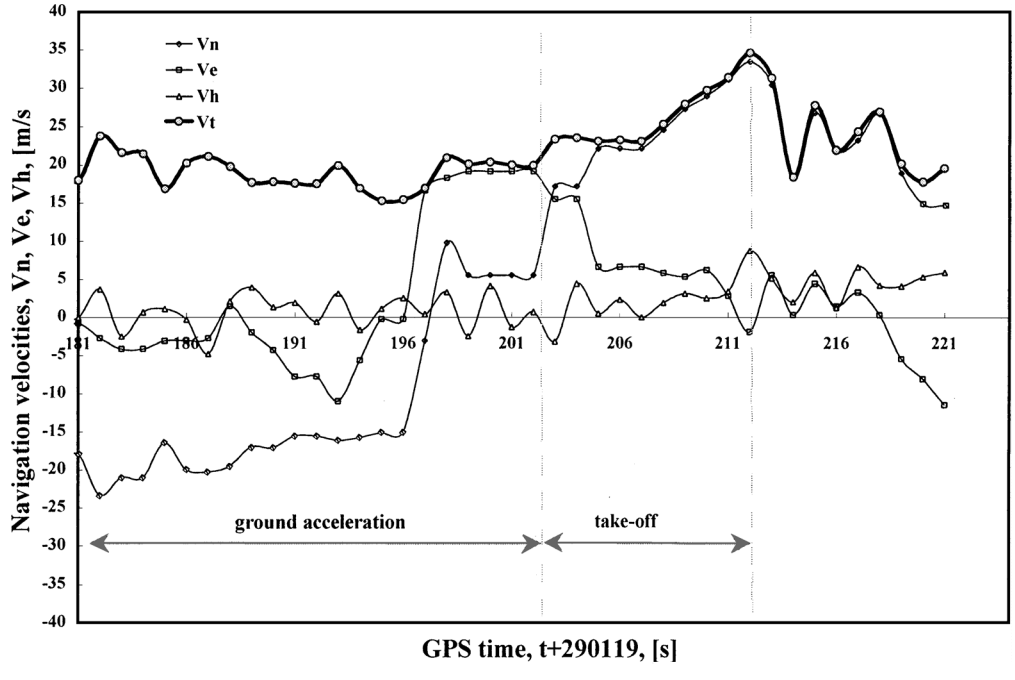

Fig. 4 Navigation velocity detected by Svy II DGPS for the OS-60 RPV at takeoff condition.

Static DGPS Accuracy Test

For higher accuracy requirement, the static DGPS positioning performance and least-square DGPS postprocessing program are further studied. These three GPS receivers are now managed to collect the real-time pseudorange data for a period of 2 h. Figure 2 and Table 2 summarize the results of the measured DGPS static positioning and velocity accuracy, where the effects from the GPS Position Dilution of Precision (PDOP) and space vehicle (SV) are essentially neglected. The measured rms values of the two-dimensional position accuracy of Svy II and XL-25 are 4.12 and 3.78 m, respectively. In addition, the corresponding three-dimensional position rms accuracy values are 4.93 and 5.67 m, respectively, for both receivers. However, the high-accuracy, high-cost GPS Z-12 receiver can provide two- and three-dimensional position rms accuracy to the levels of 0.24 and 0.35 m, respectively. The accuracy levels of the static navigation velocity for the three GPS receivers are shown in Table 2 for comparison. Their resulting rms accuracy values are 1.12 (Svy II), 0.08 (XL-25), and 0.0013 m/s (Z-12). Note that by

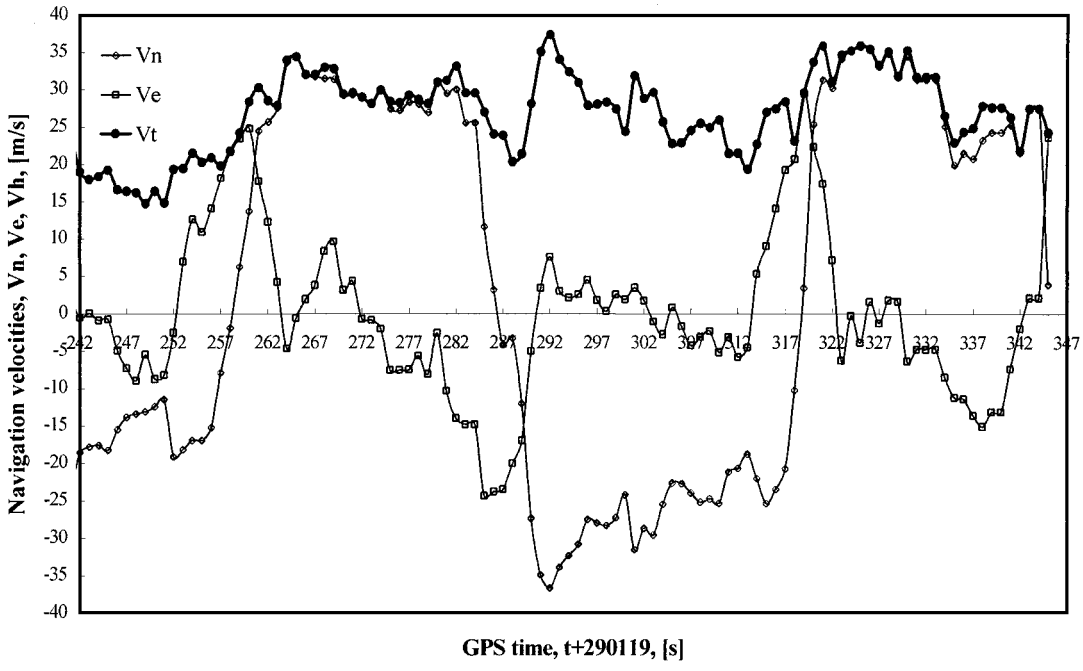

Fig. 6 Navigation velocity detected by Svy II DGPS for the OS-60 RPV at cruise condition.

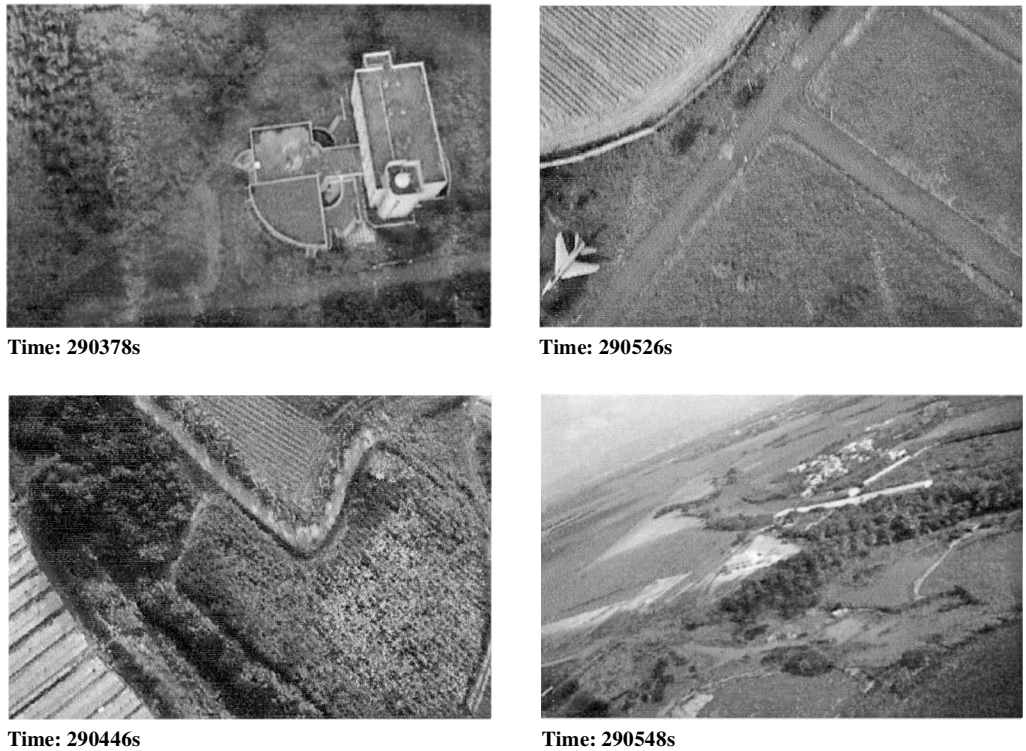

Time: 290378s **Time: 290526s**

Time: 290446s **Time: 290548s**

Fig. 7 Aerial photographs/images using DC-40 digital camera on the OS-60 RPV with synchronized Svy II DGPS position information.

applying the L1 carrier phase smoothing technique, the XL-25 velocity accuracy can then achieve a decimeter level in comparison with the 1-cm level obtained from the Z-12 receiver.

Svy II Receiver Flight Test on OS-60 RPV

After the static performance verification of all GPS used on the ground, the Svy II receiver and DC-40 digital camera are then integrated as a payload module, which is carried on the OS-60 RPV for the flight test. Before the flight test starts, the timing system of DC-40 for taking photographs/images is adjusted to match the GPS time such that the two cameras can be synchronously triggered. The photographs/images are then used in comparison with the GPS spatial and positional navigation solutions. The detected airborne pseudorange data and the digitized aerial images are recorded in the RAM memory for postflight processing. The GCS synchronously records the pseudorange data and the triggering time of the fixed station GPS so as to monitor the operation of the air photography of the DC-40 camera.

Figures 3 and 4 show the three-dimensional trajectory and the related navigation velocity of the OS-60 RPV in the takeoff condition, which includes ground acceleration, nose wheel liftoff, climbing, and turning motion. Recall that the rms accuracy values of position and velocity for the Svy II receiver are 3.87 m and 1.12 m/s, respectively. However, the results appear to be poor at flight altitude measurement, which shows higher deviation of the DGPS altitude solution. While in the cruising condition with the engine throttle kept constant, the cruise flight path and navigation velocity solutions of the OS-60 RPV are shown in Figs. 5 and 6. The downlinked flight information indicates that the output engine horsepower is

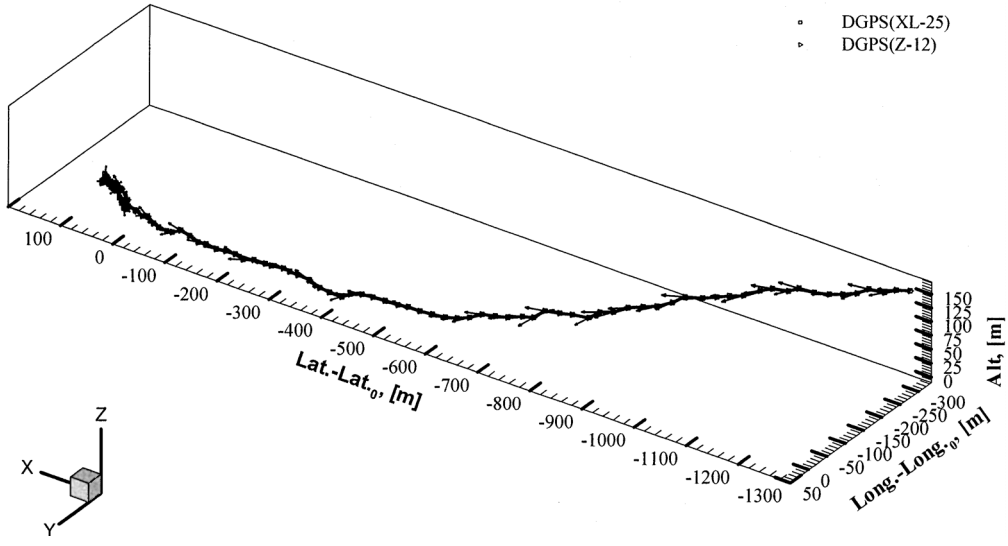

Fig. 8 Comparison of the flight trajectories detected by XL-25 and Z-12 for the MXLII ultralight airplane at landing condition.

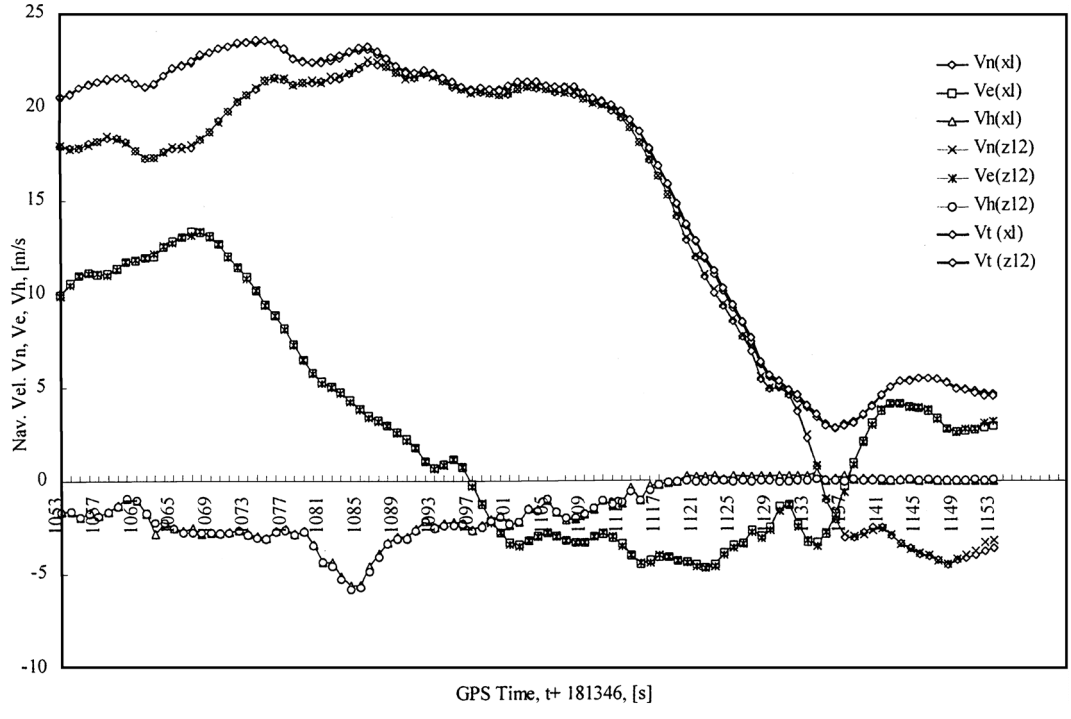

Fig. 9 Comparison of the navigation velocity detected by XL-25 and Z-12 for the MXLII ultralight airplane at landing condition.

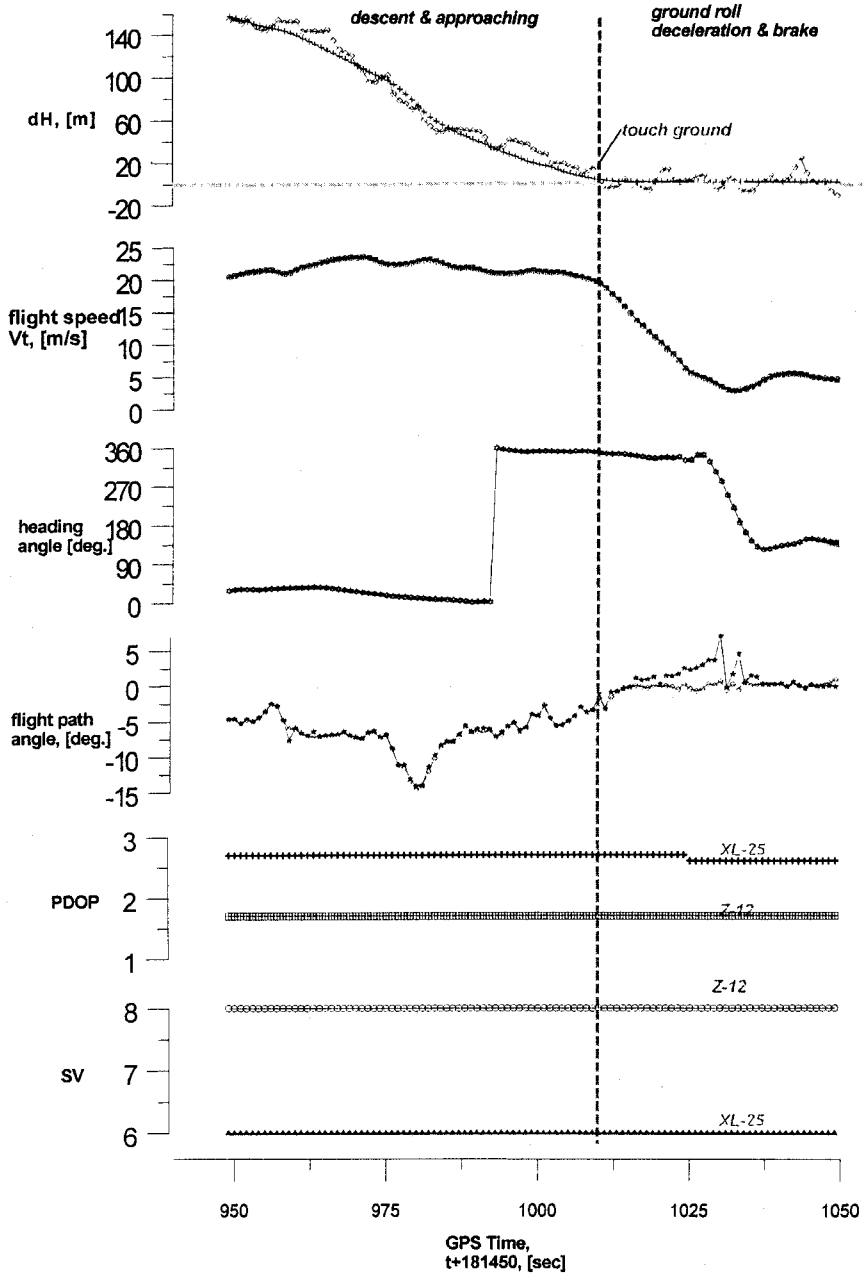

Fig. 10 Comparison of the dynamic DGPS solutions detected by XL-25 and Z-12 for the MXLII ultralight airplane at landing condition.

about 1.6 hp and the flight velocity varies between 25 and 30 m/s during the cruise. As a matter of fact, the higher multipath errors occur at the takeoff than that at the cruise flight. This is due to the less visible GPS numbers acquired during the flight test. That is, the PDOP and GPS visible numbers at takeoff and cruise conditions are (3.2, 5) and (2.8, 6), respectively, at the flight test. For the landing condition, the flight altitude and velocity are significantly influenced by the multipath interference. After the RPV touches down and decelerates to a complete stop, the standard deviation of the vertical velocity V_h is measured again to be about 0.4 m/s.

The aerial photographs/images taken from the DC-40 camera are shown in Fig. 7, which contains the relative position information of the Svy II DGPS in the form: GPS time, E, N, ϕ, λ, h, X, Y, and Z. The present aerial-photography images with the detected multicoordinate information appear to be useful in the GPS/Geodetic Information System (GIS) application. Note that the total cost of the aerial-photography payload plus the GPS receiver in the present system is much lower than the commercial systems cost from U.S.$3000 to U.S.$8000. Based on the onboard payload listed in Table 1, the self-developed payload can be operated in both postprocessing and real-time modes. On the downlink mode, the real-time GPS system should be equipped with the Terminal Node Controller (TNC) radio modem. However, only U.S.$1950 and U.S.$1200 are needed for the two modes. Therefore, the present aerial-photography/DGPS payload system cannot only be used in academic research and near-ground surveillance, but also be used as a valuable navigation sensor and remote sensing payload for UAVs.

XL-25 and Z-12 Flight Tests on MXLII Ultralight Airplane

To compare the relative kinematic DGPS accuracy between the low cost XL-25 receiver and the high-end Z-12 receiver, MXLII ultralight airplane is used for the flight test. Two antennas are mounted side by side on the main wing of the airplane for the two receivers. This test is mainly focused on the DGPS relative accuracy at various flight conditions. The GPS pseudorange data and the digitized aerial images are recorded onboard in flash RAM for postflight processing. Meanwhile, the GCS synchronously records the GPS fixed station

pseudorange data. Figure 8 shows the flight trajectory of the MXLII airplane at the landing condition. Before touching down, the flight-path angle of the airplane maintains about 5 deg in descent. During the decelerating and braking on the ground, the relative accuracy of the flight-path angle from XL-25 appears to be worse than that of Z-12. The detected navigation velocities from the XL-25 and Z-12 receivers are compared in Fig. 9. Note that the XL-25 DGPS can perform up to 0.5 m/s of velocity accuracy, whereas the Z-12 DGPS can attain the level of 0.1 m/s. Their relative differences of the rms velocity accuracy in the north–east–down frame are 0.3, 0.2, and 0.29 m/s, respectively.

With the use of the Z-12 DGPS solution as the baseline, the positioning performance of the XL-25 DGPS is further evaluated. Figure 10 shows the dynamic DGPS solutions for XL-25 and Z-12 receivers onboard the MXLII airplane at the landing condition. The results indicate that the relative deviations of the two- and three-dimensional rms positioning accuracy are 2.42 and 2.6 m, respectively. The relative rms accuracy differences of heading angle and flight-path angle are 0.86 and 3.05 deg. It appears that the present flight-test results show good agreement with the high-end precise DGPS accuracy, which is also obtained by James.[12] As a result, the smoothed pseudorange XL-25 DGPS solution cannot only provide reliable navigation velocity data, but also is attractive for use as a low-cost compass. Note that both Z-12 and XL-25 GPS antennas are arranged at the same conditions, except that the Z-12 antenna is of the geodetic double-band type and the XL-25 uses the L1 patch-type antenna. During the flight test, the XL-25 receiver has an SV value of 8 and PDOP of 2.2, while the Z-12 receiver has the SV value of 8 and PDOP of 1.9. The deviations are mainly a result of the XL-25 being masked about 5 deg of the elevation angle, whereas the Z-12 can be set to only 1 deg.

Concluding Remarks

A low-cost, high-accuracy differential GPS/aerial-photography payload is developed and flight tested on an OS-60 RPV and an MXLII ultralight airplane. Three different types of commercial GPS are used in the investigations. Results indicate that the static DGPS position accuracy for the low-cost C/A DGPS receivers, i.e., Svy II and XL-25, can attain 10 m at a 95% confidence level, and static navigation velocity errors are 2.2 and 0.17 m/s, respectively. However, the high-end Z-12 receiver can provide 3.5-m and 0.02-m/s accuracy in the relative static survey mode. With the aid of the carrier phase smoothing technique, the card-type, easily integrated C/A code XL-25 GPS receiver can effectively improve its navigation velocity and heading angle solutions. The flight-test results reveal that the deviations of the relative rms accuracy for the three-dimensional position and flight velocity between XL-25 and Z-12 are well below 2.6 m and 0.5 m/s, respectively. The detected heading angle and flight-path angle can also be controlled to an accuracy level of 1 and 3 deg, respectively. The present DGPS/aerial-photograph payload, which combines the conventional digital camera and the low-cost DGPS module, can be cost effectively applied in both real- or nonreal-time navigation investigations. Moreover, only a cost of U.S.$2000 is required to develop such a reliable and easy-to-install payload system for RPV applications.

Acknowledgment

This work is supported by National Science Council under the Contract NSC 88-2612-E-006-001.

References

[1]Mcghee, R. B., and Clynch, J. R., "An Experimental Study of an Integrated GPS/INS System for Shallow-Water AUV Navigation (SANS)," *Proceedings of the Ninth Symposium on Unmanned Submersible Technology*, Monterey, CA, Sept. 1995, pp. 1–10.

[2]John, J. D., Hossny, N. Y., and Hohman, D. S., "Use of the Global Positioning System for Evaluating Inertial Measurement Unit Errors," *Journal of Guidance, Control, and Dynamics*, Vol. 17, No. 3, 1994, pp. 435–441.

[3]Cannon, M. E., "DGPS Kinematic Carrier Phase Signal Simulation Analysis for Precise Velocity and Position Determination," *Proceedings of the National Technical Meeting for Institute of Navigation*, Jan. 1997, pp. 335–350.

[4]Parkinson, B. W., "Origins, Evolution, and Future of Satellite Navigation," *Journal of Guidance, Control, and Dynamics*, Vol. 20, No. 1, 1997, pp. 11–25.

[5]Sun, X., Xu, C., and Wang, Y., "Analysis of Flight-path Deviation for Navigation of Unmanned Space Vehicle by GPS," *Proceedings 1996 International Conference on GPS*, Inst. for Information Industry, Taipei, 1996, pp. 159–160.

[6]Sturz, R. A., and Hansen, B. J., "Payload Considerations for RPV/UAV Application," *Proceedings of the SPIE Airborne Reconnaissance XIII*, edited by P. A. Henkel, F. R. LaGesse, and W. W. Schurter, Vol. 1156, 1989, pp. 45–48.

[7]Swift, G., Sebak, K., and Shepard, C., "Subsonic Unmanned Air Reconnaissance System Design," *Proceedings of the AIAA/AHS/ASEE Aircraft Design, Systems and Operations Conference*, AIAA Paper 90-3281-CP, AIAA, Reston, VA, Sept. 1990.

[8]Baeder, B. T., and Rhea, J. L., "GPS Attitude Determination Analysis for UAV," Society of Photo–Optical Instrumentation Engineers, Vol. 2738, 1996, pp. 232–243.

[9]"UAV Annual Report-1996," Defence Airborne Reconnaissance Office, Pt. 1–4, Sept. 1997, pp. 1–45.

[10]Montgometry, P. Y., "Carrier Differential GPS as a Sensor for Automatic Control," Ph.D. Thesis, Dept. of Aeronautics and Astronautics, Stanford Univ., Stanford, CA, 1996.

[11]Guan, W. L., Hsiao, F. B., and Ho, C. S., "Developing a GPS Navigation System for Remotely Piloted Vehicle," *Proceedings of the AIAA Guidance, Navigation, and Control Conference*, AIAA-97-3693, AIAA, Reston, VA, 1997, pp. 1782–1790.

[12]James, R., "GPS and Differential GPS: An Error Model for Sensor Simulation," *IEEE Transactions on Aerospace and Electronics Systems*, 1994, pp. 260–266.